

Monte Carlo Simulations of the Two-Dimensional Two-Component Plasma on a Line

G. Manificat¹ and J. M. Caillol¹

Received July 2, 1993

We study by means of Monte Carlo simulations the Kosterlitz–Thouless transition for the two-dimensional, two-component plasma confined on a line.

KEY WORDS: Coulomb systems; one dimension; Kosterlitz–Thouless phase transition; Monte Carlo simulation.

1. INTRODUCTION

Since the outstanding paper of Kosterlitz and Thouless⁽¹⁾ (KT) one has known that a two-dimensional Coulomb system, i.e., a system of particles of charge $+e$ and $-e$ interacting via a logarithmic potential $\pm e^2 \ln r$, exhibits a phase transition. This phase transition can be characterized by change in the conducting behavior of the system; at high temperatures it is conducting, whereas at low temperatures the system is a dielectric. The transition takes place at $\Gamma = \beta e^2 = 4$ for low densities. Numerical simulations on the S_2 sphere confirmed this result,⁽²⁾ indicating that, as the density grows, the transition temperature tends to decrease. The renormalization group techniques predicted this dependence.⁽³⁾ It could be conjectured from the numerical results of ref. 2 that at very high densities the transition becomes first order.

Several papers have been devoted to the study of the one-dimensional Coulomb system with a logarithmic interaction.^(4–7) Using specific discrete models, it was possible to obtain exact results at $\Gamma = 1, 2$, and 4 .⁽⁵⁾ Various methods⁽⁸⁾ indicated that the Kosterlitz–Thouless transition should occur at a value $\Gamma = 2$, independent of the particle density. In order to confirm or

¹ Laboratoire de Physique Théorique et Hautes Energies (Laboratoire associé au Centre National de la Recherche Scientifique), Université de Paris-Sud, 91405 Orsay Cedex, France.

invalidate this result, we performed Monte Carlo (MC) simulations of a one-dimensional Coulomb gas with a logarithmic interaction without any charge ordering, the model with charge ordering having been already studied.⁽⁹⁾ At first, we planned to study the strip and then to go to the line limit. Tremendous numerical difficulties limited our investigations to the line case.

Our paper is organized as follows: in Section 2 we introduce the model and a quantity needed to characterize the Kosterlitz–Thouless phase transition. In Section 3 we present and discuss our MC results and, finally we state our conclusions in Section 4.

2. THEORETICAL CONSIDERATIONS

On the two-dimensional sphere S_2 we consider particles of charge $\pm e$. On this surface the electrical potential, solution of the Poisson equation for a single charge, does not exist. Therefore, it is necessary to associate with each charge a neutralizing background of opposite total charge. We shall restrict ourselves to a system of $N/2$ hard disks of diameter σ and charge $+e$ and $N/2$ particles of the same diameter and charge $-e$. As a consequence, the neutralizing backgrounds will cancel each other. In this case, after solving the Poisson equation, the interaction energy between two particles of charge e_i and e_j on a sphere of radius R is^(2,10)

$$V(\alpha) = -e_i e_j \ln \left(\frac{2R}{L} \sin \frac{\alpha}{2} \right) \quad (2.1)$$

where L is an arbitrary length and α is the angle between the two particles. In the thermodynamic limit this system undergoes a phase transition, the celebrated Kosterlitz–Thouless phase transition. This transition is characterized by a change in the conducting behavior, which corresponds also to a modification in the long-range behavior of the correlation functions.^(11,12) At low temperatures the system is an insulator, whereas at high temperatures it becomes a conductor. A conducting system exhibits perfect screening in the sense that any infinitesimal external charge will be screened by the system. This can be characterized by various sum rules,⁽¹³⁾ notably by the Stillinger–Lovett sum rule.^(14,15) Now in order to study the one-dimensional case, we shall consider particles compelled to lie on the equator of a sphere of radius R . Let us introduce in our system an external infinitesimal linear density of charge on the equator:

$$\rho_{\text{ext}}(\varphi) = \varepsilon \cos(l\varphi) \quad (2.2)$$

where l is an integer. Then the potential created on the equator by this distribution of the charge is

$$\Phi(\varphi) = \frac{\pi R \varepsilon}{l} \cos(l\varphi) \quad (2.3)$$

Now, if the system is conducting, it should screen perfectly this external charge. Using linear response theory, we get the excess charge density created by this external density of charge:

$$\begin{aligned} \rho_{\text{exc}}(\varphi) &= -\beta R \left\langle \hat{\rho}(\varphi) \int \hat{\rho}(\varphi') \Phi(\varphi') d\varphi' \right\rangle \\ &= -\frac{\beta \pi R^2}{l} \varepsilon \left\langle \hat{\rho}(\varphi) \int \hat{\rho}(\varphi') \cos(l\varphi') d\varphi' \right\rangle \end{aligned} \quad (2.4)$$

where β is the inverse temperature and $\hat{\rho}(\varphi)$ is the microscopic charge density at angle φ . We should have

$$\rho_{\text{exc}}(\varphi) = -\rho_{\text{ext}}(\varphi) = -\varepsilon \cos(l\varphi) \quad (2.5)$$

so

$$\int \rho_{\text{exc}}(\varphi) \cos(l\varphi) d\varphi = -\pi \varepsilon \quad (2.6)$$

and

$$\frac{\beta R^2}{l} \left\langle \int \hat{\rho}(\varphi) \cos(l\varphi) d\varphi \int \hat{\rho}(\varphi') \cos(l\varphi') d\varphi' \right\rangle = 1 \quad (2.7)$$

So, denoting by e_i and φ_i the charge and position of the i th charge, respectively, we finally get

$$\frac{\beta}{l} \left\langle \left[\sum_i e_i \cos(l\varphi_i) \right]^2 \right\rangle = \mathbf{m}_l^2 = 1 \quad (2.8)$$

It is also necessary to define the constant E_0 to be added to the Hamiltonian, in order to fix the zero of energy. A convenient choice is⁽²⁾

$$E_0 = \frac{\Gamma}{4} \left[\ln(2) + 2 \ln \frac{R}{\sigma} \right] \quad (2.9)$$

where σ is the size of the hard rods.

It will prove useful to calculate the analytical expression of the \mathbf{m}_l^2 for a system of two particles of opposite charge

$$\mathbf{m}_l^2 = \frac{\Gamma}{l} \langle [\cos(l\varphi_1) - \cos(l\varphi_2)]^2 \rangle$$

where φ_1 and φ_2 are the respective positions of the particles. If we define $\lambda = \pi\rho\sigma/2$, where ρ is the average macroscopic density of particles of both types, it is possible to derive the following expressions for, e.g., $l = 1$ and 3:

$$\mathbf{m}_1^2 = \Gamma \frac{\int_{\lambda}^{\pi/2} du |\sin u|^{-\Gamma+2}}{\int_{\lambda}^{\pi/2} du |\sin u|^{-\Gamma}} \times \left(2 + \frac{\sin 2\lambda}{\pi - \lambda} \right) \quad (2.10a)$$

$$\begin{aligned} \mathbf{m}_3^2 &= \frac{2\Gamma}{3(\pi - \lambda)} \\ &\times \frac{[9 \int_{\lambda}^{\pi/2} du |\sin u|^{-\Gamma+2} + 16 \int_{\lambda}^{\pi/2} du |\sin u|^{-\Gamma+6} - 24 \int_{\lambda}^{\pi/2} du |\sin u|^{-\Gamma+4}]}{\int_{\lambda}^{\pi/2} du |\sin u|^{-\Gamma}} \\ &\times \left(\pi - \lambda + \frac{1}{6} \sin 6\lambda \right) \end{aligned} \quad (2.10b)$$

3. MC SIMULATIONS

We present here the results of MC simulations performed in the canonical ensemble. We studied the two isochores $\rho^* = (N/2\pi R)\sigma = 0.01$ and $\rho^* = 0.1$ for values of the coupling parameter ranging from $\Gamma = 0.5$ up to $\Gamma = 3$. We paid particular attention to finite-size effects by performing several series of simulations with different numbers N of particles (i.e., $N = 50, 100$, and 200). This study of the influence of N on the results was supplemented by the analytical results of Section 2 concerning systems of $N = 2$ particles. For each considered state we computed the internal energy βu and the fluctuations \mathbf{m}_l^2 (for $l = 1, 2, \dots, 5$).

In our first attempts we used the standard Metropolis algorithm⁽¹⁶⁾ and we encountered unexpected numerical difficulties linked with a very slow convergence of the simulation in the transition region. It may be useful to recall that in a standard MC simulation of a fluid system a trial configuration of the Markov chain is obtained by selecting a particle of the system and displacing it by amounts Δx —for 1D systems—randomly and uniformly distributed in the interval $[-\xi, +\xi]$. ξ is a parameter of the calculation chosen so as to ensure a rapid convergence of the simulation. Usually ξ is a fraction of some characteristic length attached to the system—for instance, σ for dense, hard spheres. In the present case, however, a

finite proportion of positive and negative charges tend to form neutral dipolar pairs and the microscopic configurations of the system are characterized by two distinct characteristic lengths: the size of the dipolar clusters—of the order of σ —on one hand, and the mean distance between free particles and (or) dipolar clusters in the other hand—of the order of $1/\rho^*$. At the low densities considered in this work the latter is much larger than the former and the standard sampling procedure works badly. Indeed, in order to sample efficiently the clusters, one is led to choose a small value for ξ ($\xi \sim \sigma$) and consequently the relative displacements of the free particles and the dipolar clusters are very slow. An unexpected consequence is that if the system happens to acquire a net polarization $\mathbf{m} = \sum_i q_i \mathbf{r}_i$ in a given configuration of the Markov chain it takes thousands of MC steps to relax to a state of zero polarization. Moreover, in these polarized states the values of the internal energy βu and the order parameters \mathbf{m}_i^2 are strongly affected by the polarization and the convergence of these quantities toward their equilibrium values is very slow and demands a prohibitive amount of CPU time.

In order to circumvent this difficulty, we developed a new algorithm very similar to the one used by Hansen and Viot in their MC study of the 2D Coulomb gas of point charges ($\Gamma < 2$).⁽¹⁷⁾ In our procedure the positive and negative charges are classified into neutral pairs periodically in the course of the calculation. Then we consider two types of trial displacements: let us call them “plasma” and “dielectric” displacements. A dielectric displacement concerns a pair and it is made in two steps: first, the two charges of the pairs are displaced by the same amount $\Delta x_+ = \Delta x_- \sim 1/\rho^*$, and second one considers two small displacements $\Delta x_+ = -\Delta x_- \sim \sigma$ aimed at sampling the dipole strength of the pair. A “plasma” displacement concerns individual particles and is defined as usual; it is aimed at breaking the pairs into free particles. The relative frequency of these two types of displacement was chosen so as to speed up the convergence of the calculations. For several points we checked that the results were indeed independent of the various parameters—*a priori* displacements ξ , relative frequency of the two kinds of displacements, etc.—of the simulation procedure.

This new algorithm greatly facilitated the convergence of an MC simulation, but it did not remove all the numerical difficulties. Probably the difficulties are linked with the occurrence of an algebraic ($\sim 1/r^2$) decay of the correlation in the conducting phase as indicated by the theoretical prediction for discrete versions of the model.^(4,5) We observed that for the lowest considered density ($\rho^* = 0.01$) and for a few states in the transition region the system acquires spontaneously a net polarization at some step of the Markov chain and remains trapped in this polarized state during thousands of MC steps. Faced with this quasi-insurmountable difficulty, we

Table I. MC Results for the Isochore $\rho^* = 0.01^a$

Γ	N	$N_{st}(10^5)$	βu	m_1^2	m_2^2	m_3^2	m_4^2	m_5^2
0.5	50	3.5	0.898 (1)	0.92 (2)	0.85 (1)	0.79 (1)	0.75 (1)	0.70 (1)
0.5	100	1.0	0.896 (9)	0.89 (6)	0.95 (5)	0.89 (4)	0.87 (3)	0.81 (3)
0.5	200	0.5	0.904 (1)	1.0 (1)	1.01 (7)	0.90 (4)	0.94 (4)	0.86 (3)
0.7	50	2.5	1.113 (1)	0.94 (2)	0.87 (1)	0.83 (1)	0.78 (1)	0.74 (1)
0.7	100	1.0	1.113 (1)	1.03 (9)	0.92 (5)	0.89 (4)	0.85 (4)	0.82 (2)
1.0	50	2.5	1.300 (2)	0.93 (2)	0.86 (1)	0.80 (1)	0.76 (1)	0.72 (1)
1.0	200	0.5	1.308 (2)	0.91 (8)	0.89 (6)	0.95 (5)	0.90 (4)	0.94 (8)
1.1	50	2.5	1.322 (2)	0.89 (2)	0.83 (2)	0.77 (1)	0.72 (1)	0.68 (1)
1.2	50	2.5	1.324 (3)	0.84 (4)	0.78 (3)	0.71 (2)	0.68 (2)	0.62 (1)
1.2	200	1	1.331 (3)	0.97 (8)	0.93 (6)	0.89 (4)	0.87 (3)	0.84 (3)
1.3	50	5.0	1.288 (4)	0.73 (6)	0.65 (3)	0.60 (2)	0.56 (2)	0.53 (2)
1.3	100	10.0	1.216 (5)	0.28 (5)	0.52 (6)	0.56 (6)	0.52 (5)	0.49 (4)
1.3	200	1.0	1.295 (4)	0.42 (7)	0.7 (1)	0.8 (1)	0.8 (1)	0.79 (9)
1.4	50	4.0	1.254 (6)	0.58 (6)	0.59 (5)	0.51 (3)	0.49 (2)	0.46 (2)
1.4	100	2.5	1.243 (7)	0.19 (3)	0.51 (7)	0.60 (8)	0.52 (6)	0.43 (5)
1.4	200	1.2	1.252 (6)	0.30 (6)	0.39 (6)	0.58 (9)	0.51 (8)	0.6 (1)
1.5	50	4.0	1.184 (8)	0.29 (5)	0.37 (5)	0.37 (4)	0.36 (3)	0.34 (3)
1.5	100	1.5	1.19 (1)	0.11 (2)	0.29 (6)	0.27 (4)	0.35 (5)	0.28 (5)
1.5	200	30.0	1.046 (2)	0.17 (3)	0.22 (3)	0.31 (3)	0.27 (2)	0.27 (2)
1.6	50	20.0	1.098 (5)	0.12 (2)	0.21 (3)	0.22 (2)	0.23 (2)	0.22 (3)
1.6	100	1.0	1.13 (1)	0.06 (2)	0.11 (3)	0.19 (5)	0.15 (3)	0.19 (5)
1.6	200	2.4	1.125 (6)	0.038 (3)	0.07 (1)	0.15 (2)	0.11 (2)	0.24 (3)
1.7	50	5.0	1.048 (9)	0.05 (2)	0.11 (2)	0.13 (3)	0.15 (2)	0.16 (2)
1.7	200	1.2	1.105 (9)	0.030 (7)	$7 (1) 10^{-2}$	$9 (2) 10^{-2}$	0.14 (2)	0.18 (3)
1.8	50	5.0	0.959 (9)	$2 (1) 10^{-2}$	$4 (2) 10^{-2}$	$5 (2) 10^{-2}$	$6 (2) 10^{-2}$	$8 (2) 10^{-2}$
1.8	100	0.5	1.05 (1)	$1.5 (6) 10^{-2}$	$4 (1) 10^{-2}$	$2.6 (7) 10^{-2}$	$7 (3) 10^{-2}$	$6 (2) 10^{-2}$
1.8	200	1.8	1.015 (7)	0.010 (1)	0.031 (4)	0.038 (4)	0.036 (5)	0.032 (5)
1.9	50	5.0	0.959 (9)	$3 (1) 10^{-2}$	$4 (1) 10^{-2}$	$5 (1) 10^{-2}$	$7 (2) 10^{-2}$	$8 (2) 10^{-2}$
1.9	100	1.0	1.02 (1)	$1.7 (3) 10^{-2}$	$8 (2) 10^{-2}$	$9 (3) 10^{-2}$	0.11 (2)	0.15 (3)
1.9	200	0.6	0.96 (1)	$1.4 (3) 10^{-3}$	$6 (1) 10^{-3}$	$2.9 (7) 10^{-3}$	$3.5 (7) 10^{-3}$	$1.2 (3) 10^{-2}$
2.0	50	2.0	0.81 (1)	$2 (1) 10^{-3}$	$3 (1) 10^{-3}$	$5 (2) 10^{-3}$	$7 (2) 10^{-3}$	$8 (3) 10^{-3}$
2.0	100	1.0	0.98 (1)	$6 (2) 10^{-3}$	$3.8 (9) 10^{-3}$	$1.6 (3) 10^{-2}$	$1.0 (2) 10^{-2}$	$2.4 (6) 10^{-2}$
2.0	200	0.8	0.915 (9)	$8 (1) 10^{-4}$	$3.4 (6) 10^{-3}$	$2.5 (4) 10^{-3}$	$6 (1) 10^{-3}$	$3.7 (9) 10^{-4}$
2.3	100	2.0	0.862 (8)	$1.4 (2) 10^{-3}$	$1.8 (2) 10^{-3}$	$4.6 (7) 10^{-3}$	$3.7 (5) 10^{-3}$	$6.1 (8) 10^{-3}$
2.3	200	0.5	0.83 (1)	$2.3 (6) 10^{-4}$	$6 (3) 10^{-4}$	$4 (1) 10^{-4}$	$6 (2) 10^{-4}$	$1.4 (4) 10^{-3}$
2.5	100	0.5	0.84 (2)	$1.2 (4) 10^{-3}$	$2.3 (8) 10^{-3}$	$6 (1) 10^{-3}$	$2.7 (6) 10^{-3}$	$5 (2) 10^{-3}$
2.5	200	0.2	0.81 (1)	$1.1 (4) 10^{-5}$	$4 (2) 10^{-4}$	$4 (1) 10^{-4}$	$7 (2) 10^{-4}$	$6 (2) 10^{-4}$

^a N_{st} is the number of MC steps per particle, βu is the internal energy. The m_l^2 ($l = 1, \dots, 5$) are defined in Section 2. The accuracy of the calculation was estimated by dividing the total simulation into subruns of 2×10^3 MC steps. Standard deviations were obtained from the block average. The number in parentheses, which corresponds to two standard deviations, is the accuracy of the last digit(s).

decided to discard all these polarized states from the statistical averages. This drastic and unsound—in principle—procedure has in fact a very small influence on the numerical values of the internal energy βu and the fluctuations m_l^2 for $l \gtrsim 2$, but it affects more significantly the values of $m_{l=1}^2$. In all cases very, very long runs were necessary to obtain a reliable estimate of the quantities of interest. It is quite surprising, since one of the authors did not meet such convergence problems for the 2D version of the model.⁽²⁾

The results of the simulations are summarized in Tables I and II, which correspond, respectively, to $\rho^* = 0.01$ and $\rho^* = 0.1$. For the highest density and in view of the prohibitive demand in CPU time, it was not possible to make an extensive study of size effects and we considered only systems of $N = 100$ particles. Let us discuss now our results.

3.1. $\rho^* = 0.01$

As discussed above, the reported values for $m_{l=1}^2$ are probably not conclusive; for that reason we have displayed $m_{l=3}^2$ versus Γ for various numbers of particles ($N = 2, 50, 200$) in Fig. 1. Despite very long runs, the error bars on the value of $m_{l=3}^2$ are still large; however, the behavior of the curves clearly confirms the existence of the KT transition. At a given N the fluctuation $m_{l=3}^2$ is a rapidly decreasing function of Γ . At low Γ , $m_{l=3}^2 \sim 1$ —except the case $N = 2$ (!)—and the system is in a conductive phase. At high Γ the Stillinger–Lovett condition is not verified, $m_{l=3}^2 \sim 0$, and the system is in a dielectric phase made of tightly bound pairs of charges of opposite signs. The roughening of the transition due to finite-size effects deserves a detailed discussion. In the conductive phase and for

Table II. MC Results for the Isochore $\rho^* = 0.1$ ^a

Γ	$N_{sr}(10^5)$	βu	m_1^2	m_2^2	m_3^2	m_4^2	m_5^2
1	1	0.642 (2)	0.73 (4)	0.64 (2)	0.65 (2)	0.67 (1)	0.68 (1)
1.2	1	0.727 (3)	0.80 (7)	0.82 (3)	0.81 (2)	0.83 (2)	0.83 (3)
1.4	0.8	0.748 (2)	0.70 (5)	0.69 (3)	0.72 (2)	0.73 (2)	0.75 (2)
1.5	3	0.759 (2)	0.72 (4)	0.68 (3)	0.69 (2)	0.70 (1)	0.72 (1)
1.6	4	0.767 (1)	0.67 (4)	0.67 (2)	0.67 (1)	0.67 (1)	0.69 (1)
1.7	3	0.750 (2)	0.54 (5)	0.56 (3)	0.56 (2)	0.56 (1)	0.57 (1)
1.8	2	0.750 (3)	0.52 (9)	0.48 (3)	0.50 (2)	0.52 (2)	0.53 (1)
2	3	0.688 (3)	0.20 (5)	0.29 (5)	0.32 (3)	0.33 (2)	0.34 (2)
2.1	4	0.692 (3)	0.17 (3)	0.27 (5)	0.29 (3)	0.31 (2)	0.33 (2)
2.3	4	0.759 (6)	0.18 (4)	0.40 (7)	0.54 (9)	0.48 (7)	0.55 (6)
2.4	4	0.748 (6)	0.14 (3)	0.23 (5)	0.32 (6)	0.40 (7)	0.43 (6)

^a See footnote to Table I for key.

$\Gamma \lesssim 1.5$, $\mathbf{m}_{l=3}^2$ takes values significantly smaller than 1 and which are increasing functions of the number N of particles. This is an expected result; perfect screening—corresponding to the theoretical value $\mathbf{m}_{l=3}^2 = 1$ —can only occur if the correlation length is much smaller than the size of the system, i.e., for very large systems near the critical point. As apparent in Fig. 1, $\mathbf{m}_{l=3}^2$ is a decreasing function of N for $\Gamma \gtrsim 1.6$; this is an unexpected result. This striking feature is not compatible with a conductive phase for these values of Γ . Admittedly the large error bars on the value of $\mathbf{m}_{l=3}^2$ make illusory a quantitative study of the N dependence, but, qualitatively, our results are not compatible with a KT transition at $\Gamma = 2$. If one takes our MC results for granted and if one extrapolates them to $N = \infty$, then $\mathbf{m}_{l=3}^2$ behaves as a step function with a discontinuity at $\Gamma \approx 1.5$ – 1.6 .

Similar conclusions can be drawn from a close examination of our data for the fluctuations \mathbf{m}_l^2 , $l = 1, 2, \dots, 5$. However, our results for $\mathbf{m}_{l=1}^2$ are affected by very large numerical uncertainties and therefore they are not very conclusive. For low ($\Gamma \leq 1.3$) and large ($\Gamma \geq 1.7$) values of the coupling

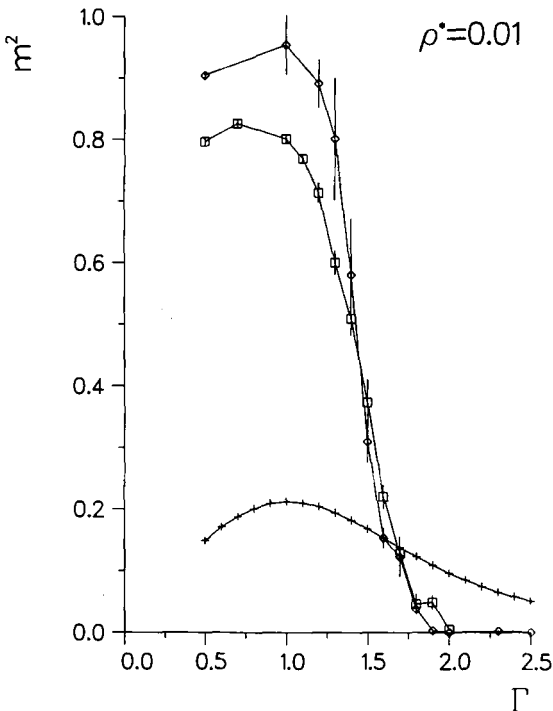


Fig. 1. $\mathbf{m}_{l=3}^2$ versus Γ for various numbers of particles at $\rho^* = 0.01$. Crosses, $N = 2$ [cf. Eq. (2.10a)]; squares, $N = 50$; diamonds, $N = 200$.

parameter all the configurations were retained and the results are not so bad. However, in the transition region $1.3 \lesssim \Gamma \lesssim 1.7$ the system can remain trapped in polarized states, which led us to exclude about 10% of the configurations. This procedure has an important effect on the numerical values of $m_{l=1}^2$ and is therefore questionable; if one admits its validity, the curve of $m_{l=1}^2$ versus Γ is very similar to the curve displayed in Fig. 1 (for $l=3$).

We conclude that at $\rho^*=0.01$ our data are compatible with a KT transition at $\Gamma \approx 1.5-1.6$.

3.2. $\rho^* = 0.1$

At this moderate density we still faced important numerical difficulties linked with a very slow convergence of the MC simulations. The MC procedure still generates metastable polarized states, but this spurious effect is less pronounced than in the case $\rho^* = 0.01$. For all the considered values of

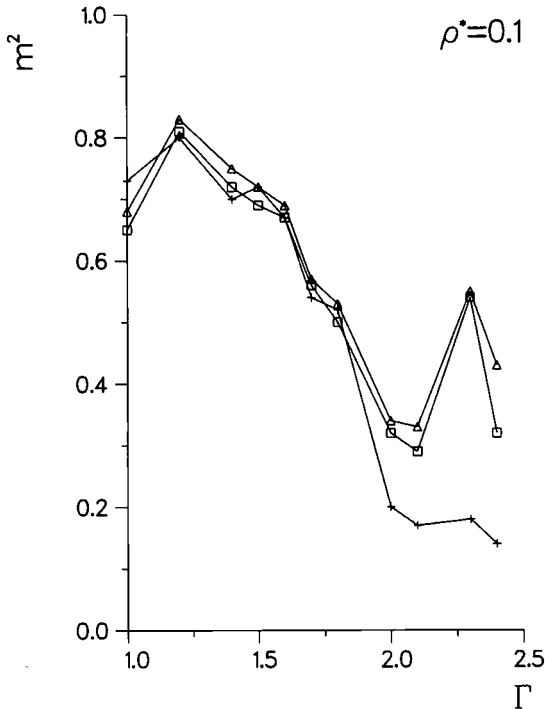


Fig. 2. m_l^2 versus Γ at $\rho^* = 0.1$ for a system of $N = 100$ particles. Crosses, $l = 1$; squares, $l = 3$; triangles, $l = 5$.

Γ very long runs were necessary in order to obtain reliable values of the energy and the fluctuations m_l^2 ($l=1, \dots, 5$). Our data are reported in Table II. In Fig. 2 we display the curves m_l^2 versus Γ for $l=1, 3, 5$ and $N=100$ particles. For $\Gamma \leq 2$ the three quantities are equal within the error bars, which is the expected behavior in a conductive phase. For $\Gamma \geq 2$ the fluctuations depend on l , which is compatible with a dielectric phase. Therefore our results at $\rho^*=0.1$ are compatible with a KT transition at $\Gamma \simeq 2$. We find for the critical coupling constant a rather large deviation at $\rho^*=0.01$ from the predicted value for zero density ($\Gamma=2$), whereas at a higher density $\rho^*=0.1$ we recover this value. Furthermore, it would indicate that between $\rho^*=0$ and $\rho^*=0.01$ the critical coupling constant decreases, as opposed to the two-dimensional case. This result is rather puzzling and we cannot draw any firm conclusions.

4. CONCLUSION

There is no contradiction between our results and the theoretical calculations. The system is a conductor at $\Gamma=1$ and an insulator at $\Gamma=2$. However, at the density $\rho^*=0.01$, despite tremendous numerical difficulties, and if one can analyze the finite-size and density effects correctly, our data seem to indicate a transition taking place at $\Gamma \approx 1.5$. In fact a MC simulation in the canonical ensemble is probably not a very appropriate way to handle our model. Relaxation times toward the equilibrium are too long. A study in another statistical ensemble (for example, the grand canonical ensemble) could well be a more efficient method to obtain results. A recent work by Kitahara on the true one-dimensional Coulomb fluid reveals also the existence of very long relaxation times for this related model.⁽¹⁸⁾

ACKNOWLEDGMENTS

We thank Prof. B. Jancovici for his interest in this work and for useful discussions.

REFERENCES

1. J. M. Kosterlitz and D. J. Thouless, *J. Phys. C* **6**:1181 (1973).
2. J. M. Caillol and D. Levesque, *Phys. Rev. B* **33**:499 (1985).
3. P. Minnhagen, *Rev. Mod. Phys.* **59**:1001 (1987).
4. P. J. Forrester, *J. Stat. Phys.* **51**:457 (1988).
5. P. J. Forrester, *J. Stat. Phys.* **42**:871 (1986).
6. H. Schultz, *J. Phys. A* **14**:3277 (1981).
7. S. A. Bulgadaev, *Phys. Lett. A* **86**:213 (1981).
8. P. J. Forrester, *J. Stat. Phys.* **60**:203 (1990).

9. K. D. Schotte and U. Schotte, *Phys. Rev. B* **4**:2228 (1971).
10. J. M. Caillol and D. Levesque, *J. Chem. Phys.* **94**:597 (1991).
11. P. A. Martin and C. Gruber, *J. Stat. Phys.* **31**:691 (1983).
12. A. Alastuey and F. Cornu, *J. Stat. Phys.* **66**:165 (1992).
13. P. A. Martin, *Rev. Mod. Phys.* **60**:1075 (1988).
14. F. H. Stillinger and P. Lovett, *J. Chem. Phys.* **48**:3858 (1968).
15. F. H. Stillinger and P. Lovett, *J. Chem. Phys.* **49**:1991 (1968).
16. M. Metropolis, A. W. Rosenbluth, M. N. Rosenbluth, A. N. Teller, and E. Teller, *J. Chem. Phys.* **21**:1087 (1953).
17. J. P. Hansen and P. Viot, *J. Stat. Phys.* **38**:823 (1985).
18. K. Kitahara, private communication.

Communicated by J. L. Lebowitz